

# TOWARD “GHOST IMAGING” WITH COSMIC RAY MUONS

**Milena D’Angelo, Augusto Garuccio, Franco Romano**, *Dipartimento Interateneo di Fisica “M.Merlin” dell’Universita degli Studi e del Politecnico di Bari and INFN Sezione di Bari, Italy*

**Francesco Di Lena**, *Dipartimento Interateneo di Fisica “M.Merlin” dell’Universita degli Studi e del Politecnico di Bari, Italy*

**Marco D’Incecco**, *INFN Laboratori Nazionali del Gran Sasso, Assergi (AQ), Italy*

**Roberto Moro, Antonietta Regano**, *Museo Storico della Fisica, Centro Studi e Ricerche E. Fermi, Roma, Italy*

**Giuliano Scarcelli**, *Harvard Medical School, Wellman Center for Photomedicine, Massachusetts General Hospital, Boston-MA, USA*

## Abstract

Optical ghost imaging is a remote imaging technique that exploits either the correlations between light beams/entangled photon pairs, or the Hanbury-Brown Twiss (Hanbury-Brown, 1974) effect typical of chaotic light sources. Is it possible to implement ghost imaging with massive particles? The Extreme Energy Events (EEE) project (Zichichi, 2005) offers a platform for attempting to answer this question. Our analysis is based on the experimental data taken in L’Aquila by two distant EEE muon telescopes (Abbrescia, 2010). Interestingly, muons from cosmic ray showers exhibit spatio-temporal correlations that offer the possibility to evaluate the feasibility of ghost imaging with massive particle.

## 1. Introduction

Ghost imaging is an optical technique that aims at gathering information on a distant object without necessity of employing imaging optics or high-resolution detectors near the object [(Belinskii, 1994), (Pittman, 1995), (Gatti, 2004) (Valencia, 2005)]. This is achieved by using two correlated beams of light: one (probe) interacts with the distant object and is revealed by a “bucket” detector, with no spatial resolution; the other (reference), in a local laboratory, goes through imaging optics and is detected by a high spatial resolution detector. The correlation between the two beams allows revealing the structure of the object, remotely, from a coincidence measurement between the two detectors. Due to this property, optical ghost imaging has recently emerged as a promising low-light-level remote sensing tool [(Meyers, 2008), (Scarcelli, 2009), (Brida, 2010)].

The main idea of the present paper is to trace the way toward the implementation of the ghost imaging protocol using correlated massive particles instead of light beams. Muons generated by cosmic rays are an interesting source to study in the context of ghost imaging: As naturally available deeply penetrating particles characterized by an extremely small De Broglie wavelength, they are promising candidates for long distance high resolution ghost imaging.

The project Extreme Energy Events (EEE) (Zichichi, 2005) offers a platform for studying the feasibility of ghost imaging with cosmic ray muons. Muon “telescopes” composed of three Multigap Resistive Plate Chambers (MRPC) [(Akindinov, 2000), (Abbrescia, 2008)], have been built and installed in many high schools across Italy. Some of them are already in operation and coincidence detection between muons have been measured in two neighbor schools of L’Aquila, 180m apart [(Regano, 2009), (Abbrescia, 2010)]. Our analysis is based on the experimental data taken for 9 days in L’Aquila.

In this paper, we start with a brief review of quantum imaging, by introducing the ghost imaging experiments based on both entangled [(Belinskii, 1994), (Pittman, 1995)] and separable systems of photons [(Bennink, 2002), (Bennink, 2004), (Howell, 2004), (D’Angelo, 2004), (D’Angelo, 2005)], as well as the ones based on chaotic light [(Gatti, 2004),(Valencia, 2005),(Ferri, 2005),(Scarcelli, 2006),(Scarcelli, 2004),(D’Angelo, Shih, 2005)]. We then introduce some basics elements of the EEE project - namely,

the detectors employed and the coincidence data so far collected [(Regano, 2009), (Abrescia, 2010)], - and enter in the core of our analysis: Extending the quantum imaging schemes to muons from cosmic rays. After studying the spatio-temporal correlation characterizing the detected muon pairs, we present a preliminary study of the feasibility of muon ghost imaging; this is an essential step toward understanding the potentialities of this naturally available source for practical applications such as remote sensing. The presented results represent the first analysis of ghost imaging with massive particles and may pave the way for the extension to particles of many other intriguing quantum optical phenomena involving classical and non-classical correlations. From a practical standpoint, the natural abundance of cosmic ray muons on earth, their long-range correlation, extremely small De Broglie wavelength and high penetrating ability would suggest this protocol as a viable way to perform very long-distance high-resolution remote imaging.

## 2. Ghost imaging with photons

The first ghost imaging experiment was realized in the mid 1990s by Pittman *et al.* (Pittman, 1995), following the theoretical proposal of Klyshko (Belinskii, 1994). By taking advantage of the strong correlation characterizing signal-idler photon pairs generated by Spontaneous Parametric Down-Conversion (SPDC) (Klyshko, 1988), Pittman *et al.* proved the possibility of reproducing the ghost image of an object, remotely. The expression “ghost” was introduced to emphasize the very peculiar nature of the phenomenon: A mask (object) is inserted in front of a bucket detector, which simply counts the SPDC signal photons transmitted by the object; the image of the mask is retrieved by recording the joint detection events of the signal-idler pairs while scanning a distant photon counting detector in the two-photon image plane, as defined on the idler beam side by the two-photon Gaussian thin lens equation:

$$\frac{1}{s_o} + \frac{1}{s_i} = \frac{1}{f}, \quad (1)$$

where  $f$  is the focal length of the lens,  $s_o$  the object-lens distance, and  $s_i$  is the “ghost” lens-image distance, given by the sum of the distances from the image to the source (i.e., the SPDC crystal) and from the source to the lens, as shown in the unfolded experimental setup of Fig.1. The single counting rates at both detectors are always fairly constant.

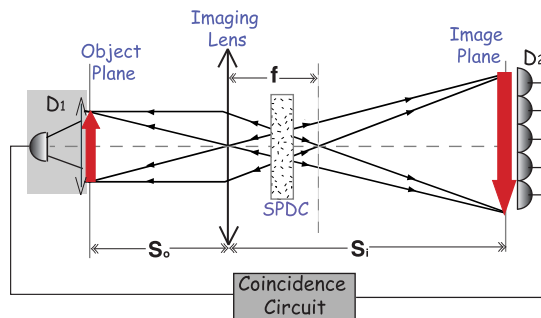


Figure 1: *Schematic representation of the unfolded experimental setup to observe ghost imaging with SPDC photon pairs: Object and imaging lens are illuminated by the signal photons, while the idlers propagate in free space; a ghost image appears when counting coincidences between the fixed bucket detector  $D_1$ , placed behind the object, and the scanning point-like detector  $D_2$ , placed in the “ghost” image plane as defined by the Gaussian two-photon thin lens equation.*

Seven years after its first discovery, an intense debate [(Gatti, 2003), (D’Angelo, 2004), (D’Angelo, 2005), (Bennink, 2004), (Howell, 2004)] was opened following an experimental work by Bennink, *et al.* (Bennink, 2002), who raised the question whether or not ghost imaging could be reproduced by classically correlated beams of light; Ref. (D’Angelo, Shih, 2005) contains a summary of this debate. A schematic representation of the experimental setup employed by Bennink, *et al.* (Bennink, 2002) is reported in Fig. 2: Pairs of light beams classically correlated in momentum are focused by two separate lenses, the object is inserted

in the focal plane of one lens, and coincidence counts are recorded between a bucket detector behind the object and a high-resolution detector placed in the focal plane of the other lens.

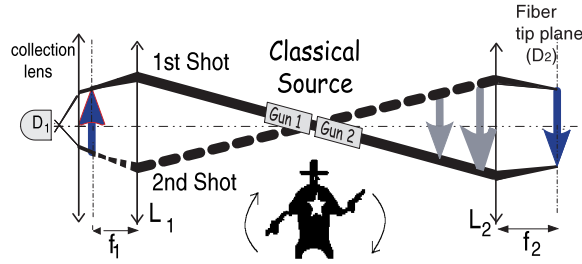


Figure 2: Schematic representation of the unfolded experimental setup for simulating ghost imaging with pairs of light beams classically correlated in momentum; the focal planes of the two lenses are required to transform the momentum correlation into the required “position” correlation.

One of the most interesting results that came out of this discussion is the possibility of producing ghost images by replacing SPDC with chaotic/thermal radiation [(Gatti, 2004), (Valencia, 2005)]: Similar to the entangled two-photon case, a two-photon Gaussian thin lens equation was found for this source (Valencia, 2005). The experimental setup is shown in Fig.3. The most evident difference with respect to the entangled case was the existence, for chaotic light, of a constant background noise accompanying the ghost image. The interpretation of the effect was soon found in terms of quantum interference, namely, coherent superposition of indistinguishable two-photon probability amplitudes (Scarcelli, 2006): the thermal ghost image was shown to exist not only when employing an imaging lens, but also in a lens-less setup, provided the object-source distance is exactly equal to the image-source distance.

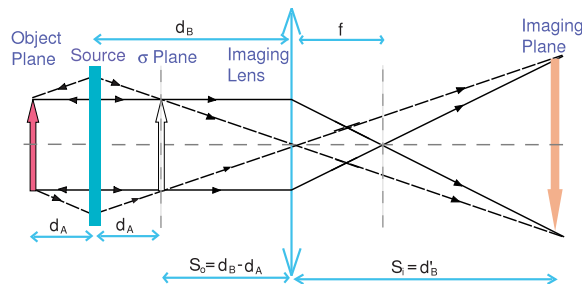


Figure 3: Schematic representation of the unfolded experimental setup for observing ghost imaging with chaotic light. A lens-less ghost image can be obtained by placing the high-resolution detector in the  $\sigma$  plane, whose distance from the source is equal to the object-source distance.

Beside its fundamental interest, quantum imaging has inspired several practical applications, from metrology (Migdall, 1999) to low-light-level remote sensing [(Meyers, 2008), (Scarcelli, 2009), (Brida, 2010)].

### 3. Cosmic ray muons and the EEE telescopes

The Extreme Energy Events (EEE) Project (Zichichi, 2005) aims at studying the extremely high energy cosmic rays by means of muon detectors (also called telescopes) distributed over an area of about  $10^6 km^2$ , in Italy. In fact, the goal is to detect the muon component of Extensive Air Showers (EAS) by measuring coincidence events between distant telescopes. Each telescope consists of three 50 cm apart Multigap Resistive Plate Chamber (MRPC) (Akindinov, 2000), gas detectors with an active area of about  $2m^2$  characterized by both time and position resolution, as well as tracking capability. As described in Ref. (Abrescia, 2010), the electric signal generated by the passage of a particle through the detector is collected by one of the 24 pick-up electrodes (160cm-long copper strips with a pitch of 3.2cm) mounted on each MRPC. The MRPC efficiency is around 95% and the time resolution is about 100ps; the absolute time

is recorded by a GPS, whose resolution is around  $60ns$  ( $\sim \sqrt{2} \sigma_{GPS}$ ). The hit strip and the difference between the signal arrival times at the strip ends enable reconstruction of the particle impact point (i.e., its  $x - y$  coordinates), with a spatial resolution of about  $2cm$  (Abbrescia, 2008). The signals detected by each MRPC are collected only when a triple coincidence of the MRPCs occurs; a triple coincidence event in the telescope thus identifies the track of the detected particle, as shown in Fig.4. Data processing allows reconstructing the muon direction with an angular resolution of about  $2^\circ$  (Abbrescia, 2008); the acceptance of the EEE telescopes is  $39^\circ$  in the plane perpendicular to the copper strips and  $58^\circ$  in the orthogonal direction.

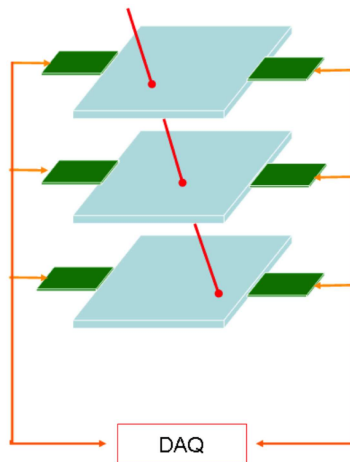


Figure 4: Sketch of the telescope employed in the EEE project. Each plane represents a MRPC; the hit points on the MRPCs allow reconstructing the track of the detected muon.

The present paper is based on the data taken for 9 effective days by two telescopes installed in two neighbor High Schools in L'Aquila,  $180m$  apart [(Regano, 2009), (Abbrescia, 2010)]. The data presented in Ref. (Abbrescia, 2010) are divided in three sets: (1) single track-single track (S-S) coincidences, where only a single track is present in each telescope; (2) single track-multihit (S-M) coincidences, where a single track in one telescope is accompanied by a multiple event, with a number of hits  $\geq 4$ , in the other telescope; (3) multihit-multihit (M-M) coincidences, where high-multiplicity events occur at both telescopes. In this paper we only consider the S-S events, namely, muon pairs detected at the two Schools, which we shall indicate as station A and B.

#### 4. Toward ghost imaging with cosmic ray muons

The existence of temporal correlation is at the heart of any ghost imaging, but of course either angular or momentum correlation are also required for guarantying the position correlation implicit in ghost images. Let us start by analyzing the temporal correlation between muons detected at the two Schools. The histogram of the time differences ( $t_A - t_B$ ) between muons detected by the two telescopes is characterized by a constant background and a peak centered around  $t_A - t_B = 0$ . Both the width of the peak and the constant background can be optimized by correcting the time differences for the average inclination ( $\theta' = (\theta_A + \theta_B)/2$ ) of the detected muon pairs with respect to the line joining the two telescopes (having length  $L$ ); the correction is implemented by replacing the detection time differences  $t_A - t_B$  with [(Regano, 2009),(Abbrescia, 2010)]:  $\Delta t = t_A - t_B \pm L \cos(\theta')/c$ . The temporal distribution of the corrected coincidence counts is reported in Fig. 5; the Gaussian fit  $a \exp[-(x - \mu)^2/2\sigma^2] + b$  gives for the peak visibility  $V = 28\%$ , for the peak width  $\sigma = 220ns$ , in agreement with the results presented in [(Regano, 2009), (Abbrescia, 2010)].

The events falling within the observed temporal correlation peak are supposed to be mostly due to muon pairs coming from the same air shower, while the constant background is due to muons coming from

different air showers. This hypothesis is strengthened by the high visibility ( $V = 93\%$ ) acquired by the temporal correlation peak as soon as one selects the events characterized by almost parallel muon tracks, namely,  $\alpha < 5^\circ$  where  $\alpha$  is the angle between muons detected at the two stations, as shown in Fig. 6. Also the peak width is somewhat reduced by the parallel track condition ( $\sigma = 180ns$ ). The highly improved visibility of this new temporal peak indicates the existence of a strong angular correlation between muon pairs belonging to the same air shower. In addition, this result indicates that the nature of the observed correlation is certainly not predominantly chaotic; in fact, chaotic identical muons propagating in the same spatial mode (such as the one selected by imposing  $\alpha < 5^\circ$ ) would produce a fermionic HBT-type dip in the temporal histogram.

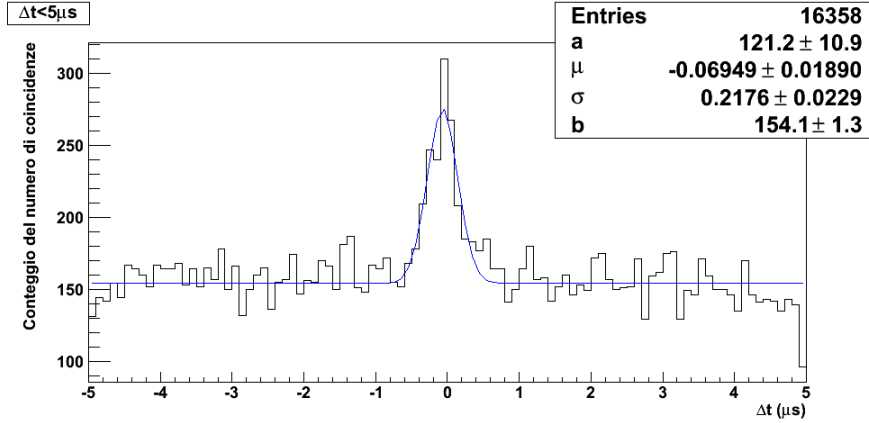


Figure 5: *Distribution of the muon pairs detected at the two Schools, A e B, as a function of the “corrected” detection time difference  $\Delta t$ . Channels are 100ns wide.*

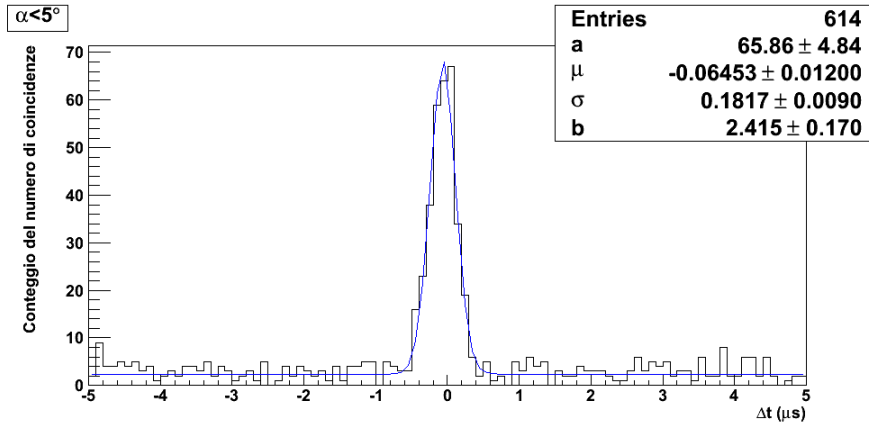


Figure 6: *Distribution of parallel muons detected at the two Schools, A e B, as a function of the “corrected” detection time difference  $\Delta t$ . Channels are 100ns wide. The condition of parallel tracks is imposed by selecting the angle between the tracks ( $\alpha$ ) to be smaller than  $5^\circ$ .*

In order to study the angular correlation between cosmic ray muons, we define a coincidence time window centered around  $\Delta t = 0$  and having total width approximately equal to the peak base (i.e.,  $4\sigma \approx 900ns$ ), and compare the angular distribution of coincident muon pairs with the angular distribution of muon pairs detected outside the coincidence window (i.e., pairs of independent muons). The results are shown in Fig. 7, where  $\theta_{A,B}$  represents the detection angle, at station A and B, respectively, with respect to the vertical direction; a common reference frame  $(x, y)$  has been defined for the two stations A and B in a plane parallel to the MRPC planes. The angular correlation (as opposed to anti-correlation) gives rise

to the distribution of the coincident muon pairs around the diagonal (as opposed to the anti-diagonal) of the  $(\theta_{Ai}, \theta_{Bi})$  planes, with  $i = x, y$ , as clearly appears from the two plots in the left column of Fig. 7. The symmetric distribution of muon pairs detected outside the coincidence window (right column in Fig. 7) indicates that independent muon pairs are neither correlated nor anti-correlated; the angular correlation characterizing coincident muon pairs is thus a pure second order effect (i.e., it is not a trivial projection of the angular distribution of independent muon pairs).

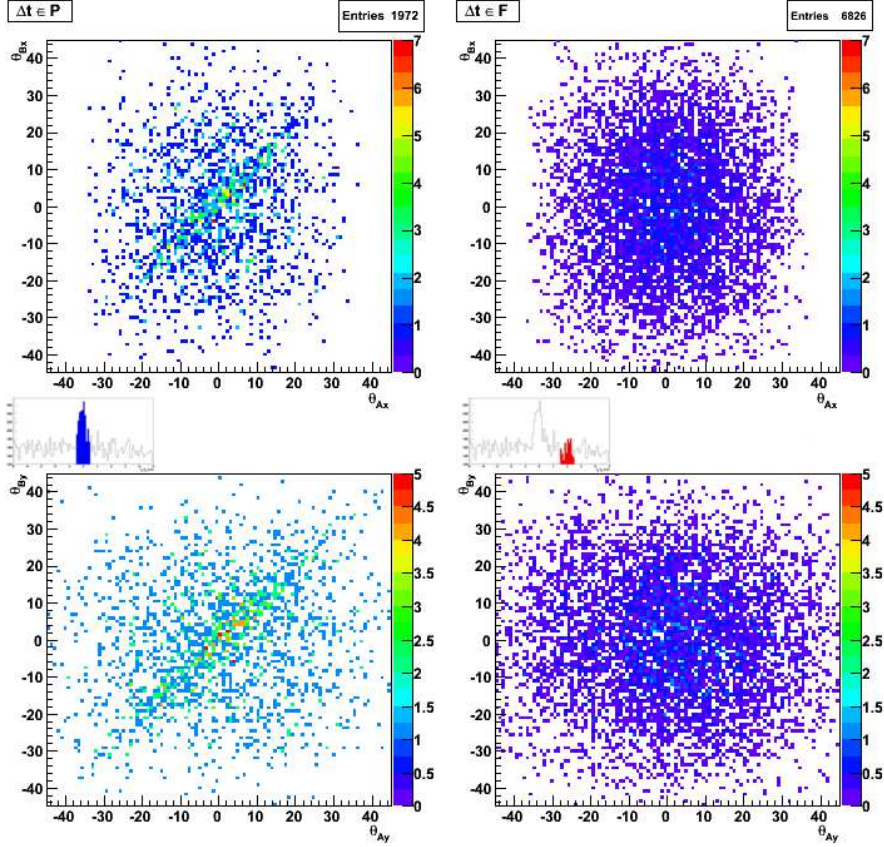


Figure 7: *Left: Distribution of the coincident muon pairs as a function of their track inclinations with respect to the vertical direction, in two orthogonal directions,  $x$  (up) and  $y$  (down), in a common reference frame for the two stations  $A$  and  $B$ . Right: Same plot for independent muon pairs, namely, muon pairs detected at the two stations far away from the temporal coincidence window. Both histograms are made of  $100 \times 100$  channels.*

The next step of is to study the possibility of extending quantum imaging schemes to cosmic ray muons. In this perspective, we exploit the discovered angular correlation to perform a preliminary feasibility study of ghost imaging with cosmic ray muons: We simulate the presence of two lenses placed on top of the two telescopes ( $A$  and  $B$ ), as schematically represented in Fig. 8, and study the position-position correlation between the focal planes of the two lenses. The possibility of simulating the presence of the two lenses comes from the knowledge of the reconstructed muon tracks: The ability of the EEE telescopes to reconstruct the tracks of the detected muons gives the angular information required to simulate the deviation a muon would have experienced if a lens was put along its path toward the telescope. In particular, the positions of the detected muons in the focal planes of the simulated lenses is simply given by  $x_{A,B} = f \tan(\theta_{A,B})$ , where  $f$  is the focal length of the two simulated lenses, and  $\theta_{A,B}$  is the incidence angle of the muons detected at station  $A$  and  $B$ , respectively; this result holds independently of the incidence positions of the detected muons, as depicted in Fig. 8.

The results obtained by simulating two lenses of focal length  $f = 10\text{cm}$  are shown in Fig. 9, where we plot the distribution of the muon pairs detected both within (blue) and outside (red) the coincidence window as a function of their relative distance  $|\rho_A - \rho_B|$  in the focal planes of the two simulated lenses. The high-visibility peak characterizing muon pairs detected in coincidence indicates that the angular correlation is naturally transformed into a position-position correlation between the focal planes of two lenses, as expected. In order to quantify such position-position correlation we normalize the distribution of the coincident muon pairs with respect to the distribution of the independent pairs (e.g., we divide the blue by the red curve) and evaluate the width of the resulting distribution by performing a gaussian fit, as shown in Fig. 9; the visibility of the resulting correlation peak is 90% and the spatial correlation in the focal plane of the simulated lenses is  $\sigma = 0.6\text{cm}$  (corresponding to an angular correlation of  $3.6^\circ$ , in agreement with an analysis performed without lenses).

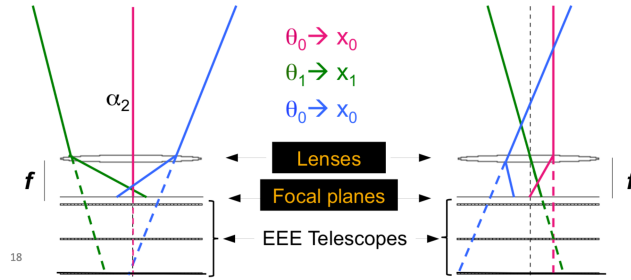


Figure 8: Schematic representation of the setup employed to study the position-position correlation: The presence of a lens of focal length  $f$  is simulated on top of each telescope, in such a way that all detected muons coming at a given angle are collected in a given point of the focal plane, independent of their position of incidence. The dashed line is the reconstructed track of detected muons; the continuous line is the track due to the simulated lens.

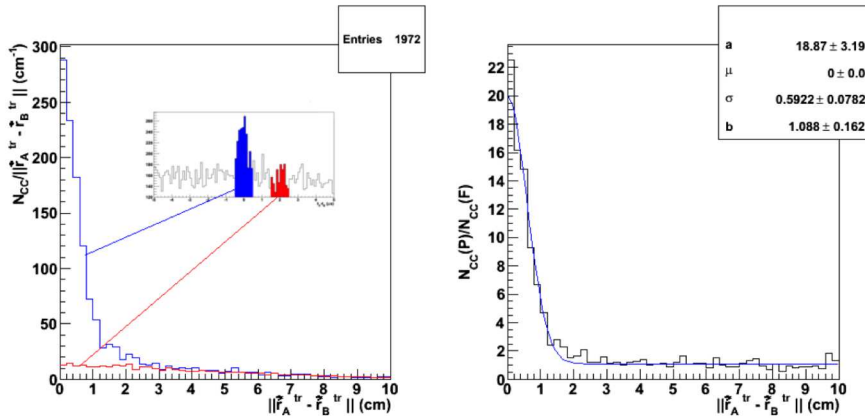


Figure 9: Left: Distribution of coincident muon pairs (blue) and independent muon pairs (red) as a function of their relative distance  $|\rho_A - \rho_B|$  in the focal planes of the two simulated lenses, having focal length  $f = 10\text{cm}$ . Right: Normalized distribution of the coincidence muon pairs as a function of their relative position in the focal planes of the simulated lenses; the continuous curve is the corresponding gaussian fit.

The existence of the position correlation between muons from extensive air shower is the building block to implement a ghost imaging scheme based on such massive particles. The result of Fig. 9 represents the point-spread-function of a ghost imaging scheme analogous to the classical version of optical ghost imaging (Fig. 2); the main difference is that we are dealing with correlated massive particles rather than with anti-correlated light beams.

## 5. Conclusion

We have reviewed both the concept of optical ghost imaging and the preliminary results of the feasibility of ghost imaging with massive particles, thus investigating the potentialities of cosmic ray muons for long-distance ghost imaging applications. The analysis has been based on the data taken in L'Aquila within the EEE project (Abbrescia, 2010).

We are currently working on the simulation of more sophisticated ghost imaging schemes, in line with the optical experiments schematically drawn in Fig. 1 and 3, by employing the same exact set of available data. This will allow both a deeper comprehension of the correlations characterizing this naturally available source of massive particles, and will indicate its potentialities in view of remote sensing applications; in fact, the results will automatically pave the way toward the extension to massive particles of many other intriguing quantum optical phenomena involving classical and non-classical correlations.

In this perspective, we are also extending the present analysis to both energy and momentum; in fact, real objects will have the potentials to be “ghostly imaged” by means of cosmic ray muons only if the strong angular correlation exploited so far is accompanied by energy correlation, thus resulting in sufficient momentum-momentum correlation between muon pairs detected in coincidence in two distant locations. The Authors sincerely thank the EEE collaboration and the “Centro Studi e Ricerche E. Fermi”, for giving us permission to analyze the data taken in L'Aquila within the EEE project; the availability of these data has been essential for conducting the present feasibility study. The Authors are particularly thankful to Marcello Abbrescia for interesting insights about the working principle of the EEE telescopes and the general setup of the EEE experiment, particularly useful in the start-up phase of the present research.

## References

- Zichichi A. (2005), La Scienza nelle Scuole, EEE-Extreme Energy Events, oral presentation at Congresso Nazionale, Societa' Italiana di Fisica (SIF), Bologna; also at [www.centrofermi.it/eee](http://www.centrofermi.it/eee).
- Abbrescia M. *et al.* (2010), *Il Nuovo Cimento* **125 B**, 243.
- Belinskii and Klyshko (1994), *JETP* **105**, 487; Klyshko D.N. (1988), *Sov. Phys. Usp.* **31**, 74.
- Pittman T.B., Shih Y.H., Strekalov D.V., and Sergienko A.V. (1995), *Phys. Rev. A* **52**, R3429.
- Gatti A. *et al.* (2004), *Phys. Rev. A* **70**, 013802.
- Valencia A., Scarcelli G., D'Angelo M. and Shih Y. (2005), *Phys. Rev. Lett.* **94**, 063601.
- Meyers R. *et al.* (2008), *Phys. Rev. A* **77**, 041801.
- Scarcelli G. (2009), *Nature Physics* **5**, 252.
- Brida G., Genovese M. and Ruo Berchera I. (2010), *Nature Photonics* **4**, 227.
- Akindinov A. *et al.* (2000), *Nucl. Instrum. Methods A* **456**, 16.
- Abbrescia M. *et al.* (2008), *Nucl. Instrum. Methods A* **593**, 263.
- Regano A. *et al.* (2009), oral presentation at XCV Congresso Nazionale, Societa' Italiana di Fisica (SIF), Bari.
- D'Angelo M., Kim Y.H., Kulik S. P., and Shih Y. H. (2004), *Phys. Rev. Lett.* **92**, 233601.
- D'Angelo M., Valencia A., Rubin M. H., Shih Y. H. (2005), *Phys. Rev. A* **72**, 013810.
- Ferri F. *et al.* (2005), *Phys. Rev. Lett.* **94** (2005) 183602; Zhang *et al.*, *Opt. Lett.* **30**, 2354.
- Scarcelli G., Berardi V., and Shih Y. (2006), *Appl. Phys. Lett.* **88**, 061106.
- Scarcelli G., Valencia A., and Shih Y. (2004), *Europhys. Lett.* **68**, 618.
- D'Angelo M., and Shih Y. H. (2005), *Laser Phys. Lett.* **2**, 567.
- Klyshko D. N. (1988), *Photon and Nonlinear Optics*, Gordon and Breach Science, New York.
- Gatti A., Brambilla E., and Lugiato L. A. (2003), *Phys. Rev. Lett.* **90**, 133603.
- Bennink R. S., Bentley S. J., Boyd R. W., and Howell J. C. (2004), *Phys. Rev. Lett.* **92**, 033601.
- Howell J. C. , Bennink R. S., Bentley S. J., and Boyd R. W. (2004), *Phys. Rev. Lett.* **92**, 210403.
- Bennink R. S., Bentley S. J., and Boyd R. W. (2002), *Phys. Rev. Lett.* **89**, 113601.
- Scarcelli G., Berardi V., and Shih Y. (2006), *Phys. Rev. Lett.* **96**, 063602.
- Migdall A. (1999), *Phys. Today* **52**, 41.
- Abbrescia M. *et al.* (2008), *Proceedings of the Cosmic Ray International Seminar (CRIS)*, Malfa, September 15-19;



to be published in Nucl. Phys. B.

Hanbury-Brown R. (1974), *Intensity Interferometer*, Taylor and Francis Ltd, London; Hanbury-Brown R. and Twiss R.Q. (1956), *Nature* **177**, 27 and **178**, 1046.